16th European Signal Processing Conference (EUSIPCO 2008), Lausanne, Switzerland, August 25-29, 2008, copyright by EURASIP

ARRAY PROCESSING FOR INTERSECTING CIRCLE RETRIEVAL

Julien Marot and Salah Bourennane

Institut Fresnel
Ecole Centrale Marseille, 13397, Marseille, France
phone: + (33) 4 91 28 27 49, fax: + (33) 4 91 28 80 67,
email: julien.marot@fresnel.fr, salah.bourennane@fresnel.fr

ABSTRACT

Circular features are commonly sought in digital image processing. SLIDE (Subspace based LIne DEtection) method proposed to estimate the center and the radius of a single circle by adapting array processing methods. Recently, a virtual circular array was proposed to estimate the radii of several concentric circles. A difficulty arises when intersecting circles are expected. In this paper, for the first time, we propose to combine linear and circular antenna, to retrieve intersecting circles. We exemplify the proposed method on a set of hand-made and real-world images.

1. REVIEW ON ARRAY PROCESSING METHODS FOR CIRCLE CHARACTERIZATION

Circular features are commonly sought in digital image processing. Circle fitting is suitable in several domains such as quality inspection for food industry, mechanical parts [1] and particle trajectories [2]. Recently, array processing methods have been adapted to this kind of problem [3]. Virtual circular and linear antenna are used to retrieve circle parameters.

1.1 Circular antenna for the estimation of several radii

We review the principles of signal generation on circular antenna. The generated signals fit classical array processing methods. Fig. 1(a) presents a binary digital image I as a square matrix of dimensions $N \times N$. Each element represents an image pixel. An object in the image is made of edge pixels with value 1, over a background of zero-valued pixels. The object is fitted by a circle with radius value r and center coordinates $(l_c,\ m_c)$. Fig. 1(b) shows a sub-image extracted from the original image, so that its top left corner is the center of the circle. This sub-image is associated with a set of polar coordinates (ρ,θ). Each pixel of the expected contour in the sub-image has the following coordinates: $r+\Delta\rho,\ \theta$. $\Delta\rho$ is the shift between the contour pixel and the circle one that fits the contour and which has the same coordinate θ.

We remind now the principles of signal generation upon a virtual circular antenna. More details about this signal generation process can be found in [3]. The basic idea is to obtain a linear phase signal from an image containing a quarter of circle. To achieve this, we use a circular antenna. A quarter of circle with radius r and a circular antenna are represented on Fig. 2. Signal generation scheme upon a circular antenna is the following: the directions adopted for signal generation are from the top left corner of the sub-image to the corresponding sensor. The antenna is composed of S sensors, so there are S signal components.

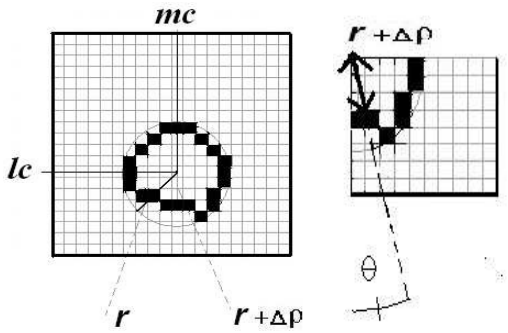

(a) (b)

Figure 1: (a) Circular-like contour; (b) Bottom right quarter of the contour and pixel coordinates in the polar system (ρ,θ) having its origin on the center of the circle. r is the radius of the circle. $\Delta\rho$ is the value of the shift between a pixel of the contour and the pixel of the circle having same coordinate θ.

Let us consider D_i, the line that makes an angle θ_i with the vertical axis and crosses the top left corner of the sub-image. The i^{th} component $(i=1,\ldots,S)$ of the signal $\mathbf{z}$ generated out of the image reads:

$$z(i)=\sum_{\substack{l,m=1\\(l,m)\in D_i}}^{l,m=N_s} I(l,m)exp(-j\mu\sqrt{l^2+m^2}), \qquad (1)$$

Most often, there exists more than one circle for one center. We demonstrate how several possibly close radius values can be estimated using a high-resolution method. To estimate the number d of concentric circles, and each radius value, we employ a variable speed propagation scheme [3]. We set $\mu=\alpha(i-1)$, for each sensor indexed by $i=1,\ldots,S$. From Eq. (1), the signal received on each sensor is:

$$z(i)=\sum_{k=1}^{d} exp(-j\alpha(i-1)r_k)+n(i),\ i=1,\ldots,S \qquad (2)$$

where $r_k,\ k=1,\ldots,d$ are the values of the radius of each circle, and $n(i)$ is a noise term due to outliers. All components $z(i)$ compose the observation vector $\mathbf{z}$. TLS-ESPRIT (Total Least Squares-EStimation of Parameters by Rotational Invariance Techniques) algorithm requires the estimation of the covariance matrix of several snapshots. There is no time-dependent signals. So the question arises as how a sample covariance matrix can be formed. This can be done

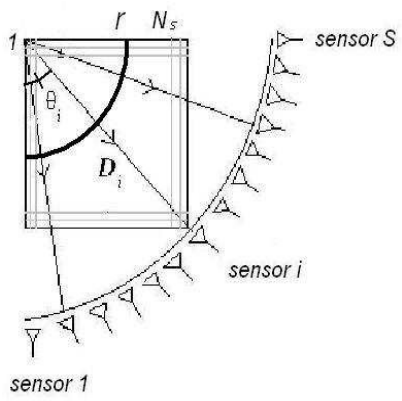

Figure 2: Sub-image, associated with a circular array composed of S sensors.

as follows [4]: From the observation vector we build K sub-vectors of length M with $d < M \leq S-d+1$: $\mathbf{z}_l = [z(l),\cdots,z(l+M-1)]^T$, $l=1,\cdots,K$. To maximize the number of snapshots [5], the first component of a snapshot is the second component of the previous snapshot. This improves the estimation of the covariance matrix that is performed in TLS-ESPRIT algorithm. We obtain then $K=S+1-M$ snapshots. Grouping all sub-vectors obtained in matrix form, we get $\mathbf{Z}_K = [\mathbf{z}_1,\cdots,\mathbf{z}_K]$, where

$$\mathbf{z}_l = \mathbf{A}_M\,\mathbf{s} + \mathbf{n}_l, \qquad l=1,\cdots,K. \tag{3}$$

$\mathbf{A}_M = [\mathbf{a}(r_1),\cdots,\mathbf{a}(r_d)]$ is a Vandermonde type matrix of size $M\times d$: the i^{th} component of $\mathbf{a}(r_k)$ is $exp(-j\alpha(i-1)r_k)$. $\mathbf{s}$ is a length d vector equal to $[1,1,\ldots,1]^T$ -superscript ^{T} denotes transpose- and $\mathbf{n}_l = [n(l),\cdots,n(l+M-1)]^T$.
The signal model of Eq. (3) suits TLS-ESPRIT method, a subspace-based method that requires the dimension of the signal subspace, that is, in this problem, the number of concentric circles. MDL criterion estimates the dimension of the signal subspace [4] from the eigenvalues of the covariance matrix.
TLS-ESPRIT is applied on the measurements collected from two overlapping sub-arrays, and falls into two parts: the covariance matrix estimation and the minimization of a total-least-squares criterion. The radius values are obtained as [4]:

$$\hat{r}_k = \frac{-1}{\alpha} Im(\ln(\frac{\lambda_k}{|\lambda_k|})),\ k=1,\ldots,d \tag{4}$$

where Im denotes imaginary part, $\{\lambda_k,\ k=1,\ldots,d\}$ are the eigenvalues of a diagonal unitary matrix. It relates the measurements from the first sub-array with the measurements resulting from the second sub-array.

1.2 Linear antenna for the estimation of circle parameters

Usually, an image contains several circles which are possibly not concentric and have different radii (see Fig. 3). To apply the proposed method, the center coordinates for each feature are required. To estimate these coordinates, we generate a signal with constant propagation parameter upon the image left and top sides. More details regarding signal generation upon a linear antenna can be found in [4]. The l^{th} signal component, generated from the l^{th} row, reads: $z_{lin}(l) = \sum_{m=1}^{N} I(l,m)exp(-j\mu m)$, where μ is the propagation parameter [4]. The non-zero sections of the signals, as seen at the left and top sides of the image (see Fig. 3), indicate the presence of features. Each non-zero section width in the left (respectively the top) side signal gives the height (respectively the width) of the corresponding expected feature. The middle of each non-zero section in the left (respectively the top) side signal yields an approximate value of the center l_c (respectively m_c) coordinate of each feature.

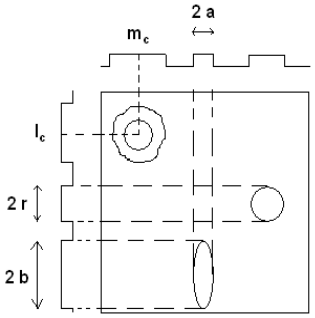

Figure 3: Model for an image containing several nearly circular or elliptic features. r is the circle radius, a and b are the axial parameters of the ellipse.

The set of methods proposed in [3] fails in retrieving intersecting circles.

2. ESTIMATION OF INTERSECTING CIRCLES BY ARRAY PROCESSING METHODS

A method which is commonly employed for the retrieval of several circles, either intersecting or not, is the generalized Hough transform (GHT). The generalized Hough transform (GHT) provides estimation of the center coordinates of circles when their radius is known [6]. Therefore the first drawback of GHT is that it requires the knowledge of the radius of all circles in the image. Another drawback of GHT is that it requires an elevated computational load.

We propose an algorithm which is based on the following remarks about the generated signals. Signal generation on linear antenna yields a signal with the following characteristics:
The maximum amplitude values of the generated signal correspond to the lines with maximum number of pixels, that is, where the tangent to the circle is either vertical or horizontal. The signal peak values are associated alternatively with one circle and another.
Signal generation on circular antenna yields a signal with the following characteristics:
If the antenna is centered on the same center as a quarter of circle which is present in the image, the signal which is generated on the antenna exhibits linear phase properties [3].
We propose a method that combines linear and circular antenna to retrieve intersecting circles. We exemplify this

method with an image containing two circles (see Fig. 4). It falls into the following parts:

- Generate a signal on a linear antenna placed at the left and bottom sides of the image;
- Associate signal peak 1 (P1) with signal peak 3 (P3), signal peak 2 (P2) with signal peak 4 (P4);
- Diameter 1 is given by the distance P1-P3, diameter 2 is given by the distance P2-P4;
- Center 1 is given by the mid point between P1 and P3, center 2 is given by the mid point between P2 and P4;
- Associate the circular antenna with a sub-image containing center 1 and P1, perform signal generation. Check the phase linearity of the generated signal;
- Associate the circular antenna with a sub-image containing center 2 and P4, perform signal generation. Check the linearity of the generated signal.

Figure 4 presents, in particular, the square sub-image to which we associate a circular antenna.

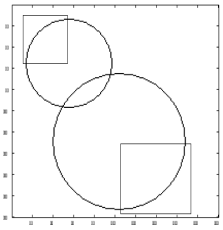

Figure 4: two intersecting circles, subimages containing center 1 and center 2.

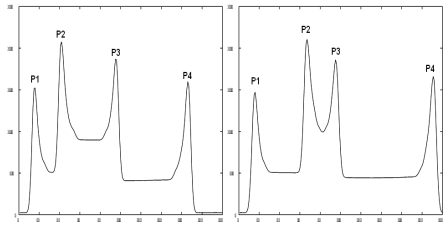

(a) (b)

Figure 5: signals generated on: (a) the bottom of the image; (b) the left side of the image.

3. RESULTS

The proposed circle fitting method is applied to images having $N = 200$ columns and rows. Then a linear antenna is composed of $N = 200$ sensors. When the circular antenna is used, the number of sensors is $S = 400$. Signal generation on linear antenna is performed with parameter $\mu = 5 \times 10^{-3}$, signal generation on circular antenna is performed with parameter $\alpha = 1.35 \times 10^{-2}$. The value $M = \sqrt{S} = 20$ for the length of each sub-array was empirically found to provide optimal results [3].
For all experiments our algorithms are run under Windows on a 3.0 Ghz Pentium 4 PC.

3.1 Hand-made images

We first exemplify the proposed method on the image of Fig. 6, from which we obtain the results of Fig. 7, which presents the signal generated on both sides of the image. The signal obtained on left side exhibits only two peak values, because the radius values are very close to each other. Therefore signal generation on linear antenna provides a rough estimate of each radius, and signal generation on circular antenna refines the estimation of both values.
The center coordinates of circles 1 and 2 are estimated as $\{l_{c1},\, m_{c1}\} = \{83,\, 41\}$ and $\{l_{c2},\, m_{c2}\} = \{83,\, 84\}$. Radius 1 is estimated as $r_1 = 24$, radius 2 is estimated as $r_2 = 30$.
The computationally dominant operations while running the algorithm are signal generation on linear and circular antenna. For this image and with the considered parameter values, the computational load required for each step is as follows:

- signal generation on linear antenna: $3.8\ 10^{-2}$ sec.;
- signal generation on circular antenna: $7.8\ 10^{-1}$ sec.

So the whole method lasts $8.1\ 10^{-1}$ sec. For sake of comparison, generalized Hough transform with prior knowledge of the radius of the expected circles lasts 2.6 sec. for each circle. Then it is 6.4 times longer than the proposed method.

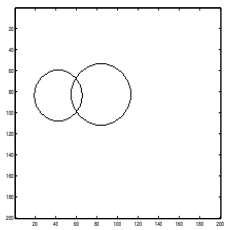

Figure 6: Processed image

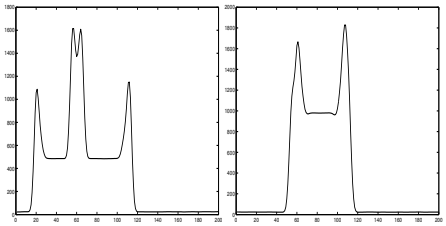

(a) (b)

Figure 7: signals generated on: (a) the bottom of the image; (b) the left side of the image.

The case presented in Figs. 8 and 9 illustrates the need for the last two steps of the proposed algorithm. Indeed the signals generated on linear antenna present the same peak coordinates as the signals generated from the image of Fig. 4. However, if a subimage is selected, and the center of the circular antenna is placed such as in Fig 4, the phase of the generated signal is not linear. Therefore, for Fig. 8, we take as the diameter values the distances P1-P4 and P2-P3. The center coordinates of circles 1 and 2 are estimated as

$\{l_{c1}, m_{c1}\} = \{68, 55\}$ and $\{l_{c2}, m_{c2}\} = \{104, 99\}$. Radius of circle 1 is estimated as $r_1 = 87$, radius of circle 2 is estimated as $r_2 = 27$.

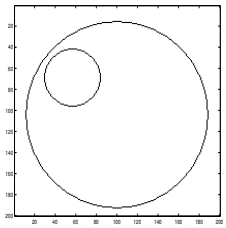

Figure 8: Processed image

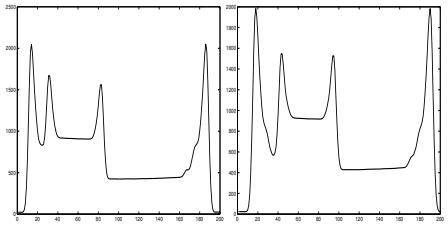

(a) (b)

Figure 9: signals generated on: (a) the bottom of the image; (b) the left side of the image.

Here was exemplified the ability of the circular antenna to distinguish between ambiguous cases.

Fig. 10 shows the results obtained with a noisy image. The percentage of noisy pixels is 15%, and noise grey level values follow Gaussian distribution with mean 0.1 and standard deviation 0.005. The presence of noisy pixels induces fluctuations in the generated signals, Figs. 10(b) and 10(c) show that the peaks that permit to characterize the expected circles are still dominant over the unexpected fluctuations. So the results obtained do not suffer the influence of noise pixels. The center coordinates of circles 1 and 2 are estimated as $\{l_{c1}, m_{c1}\} = \{131, 88\}$ and $\{l_{c2}, m_{c2}\} = \{53, 144\}$. Radius of circle 1 is estimated as $r_1 = 67$, radius of circle 2 is estimated as $r_2 = 40$.

3.2 real-world images

Fig. 11 presents the case of a real-world image. It contains one red cell and one white cell. Our goal in this application is to detect both cells. The minimum value in the signal generated on bottom side of the image corresponds to the frontier between both cells. The width of the non-zero sections on both sides of the minimum value is the diameter of each cell. Each peak value in each generated signal provides one center coordinate.

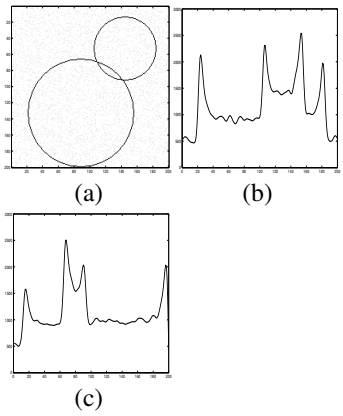

(a) (b)

(c)

Figure 10: (a) processed image; signals generated on: (b) the bottom of the image; (c) the left side of the image.

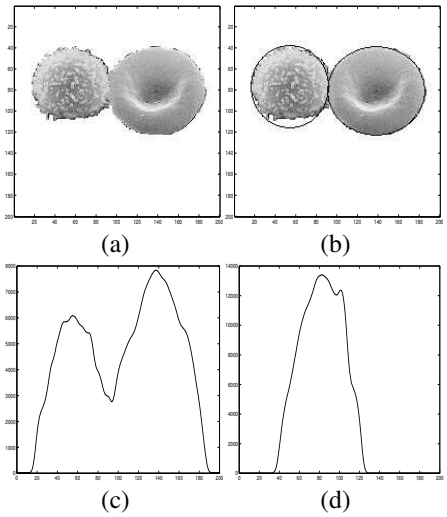

(a) (b)

(c) (d)

Figure 11: Blood cells: (a) processed image; (b) superposition processed image and result; signals generated on: (c) the bottom of the image; (d) the left side of the image.

Figures. 12 and 13 concern an astronomy imagery application. In this particular case only half circles are present in the image. As a consequence, in fig. 13(c), the non zero sections exhibit a straight edge on their left side and are slightly decreasing on the right side. The width of the non-zero sections provides the values of the radii.

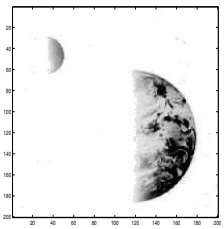

Figure 12: Processed image: Earth and moon

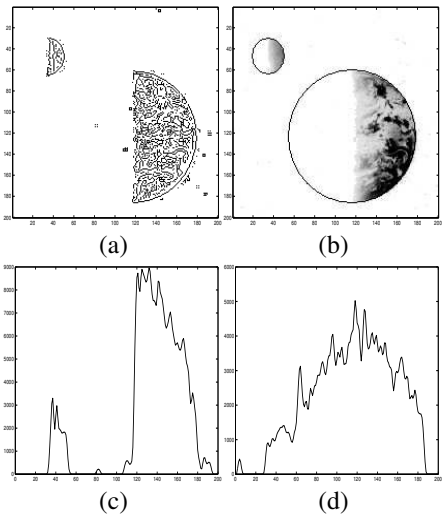

Figure 13: (a) Gradient image; superposition processed image and result; signals generated on: (c) the bottom of the image; (d) the left side of the image.

3.3 Statistical study: robustness to noise

In this subsection we study the robustness of the proposed method to noise impairment. Statistical results presented below are obtained with the image of fig. 10. Noise grey level values follow Gaussian distribution with mean and standard deviation equal respectively to 10% and 0.5% of the value of a pixel that belongs to the expected contour. The percentage of noisy pixels varies between 2% and 15%.

The performance of the proposed methods are measured by the mean error *ME* over the coordinates peaks P1, P2, P3, P4. We denote by $\hat{P}1$, $\hat{P}2$, $\hat{P}3$, $\hat{P}4$ the estimate of the coordinates of the peaks. Then *ME* is given by:

$ME = \frac{1}{4}\sum_{i=1}^{4} |\hat{P}i - Pi|$ where $|\cdot|$ means absolute value. *RMSE* is given by:

$RMSE = \sqrt{\frac{1}{4}\sum_{i=1}^{4} (|\hat{P}i - Pi|)^2}$.

The mean error and root mean square error values over the estimates of the center coordinates $\{l_{c1}, m_{c1}\}$, $\{l_{c2}, m_{c2}\}$ obtained by the GHT are defined in the same way as *ME* and *RMSE* values. Figure 14 shows the evolution of mean error and root mean square error as a function of noise percentage, for the proposed method and GHT. Error values are always less than 1 pixel.

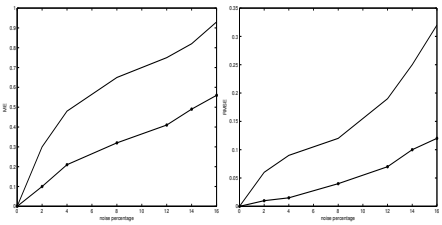

Figure 14: (a) Evolution of mean error ME as a function of noise percentage; (b) Evolution of root mean square error RMSE as a function of noise percentage. (-) Proposed method; (*-) GHT.

4. CONCLUSION

Array processing methods were adapted to contour estimation in images by a specific formalism for signal generation upon virtual antennas. For the first time, we retrieve intersecting circles, by a method based on array processing algorithms. We extend a method that was recently proposed, based on a virtual circular antenna. Signal generation on a linear antenna yields the center coordinates and radii of all circles. Circular antenna refines the estimation of the radii and distinguishes ambiguous cases. Our method outperforms generalized Hough transform in terms of computational load, we exemplified the proposed method on noisy and real-world images.

REFERENCES

[1] U. M. Landau, "Estimation of a circular arc center and its radius", *Comp. Vis. Gr. IP*, no. 38, pp. 317-26, Jun. 86.

[2] J. F. Crawford, "A noniterative method for fitting circular arcs to measured points", *Nucl. Instr. Met. Ph. Res.*, no. 211, pp. 223-25, 83.

[3] J. Marot and S. Bourennane, "Subspace-Based and DIRECT Algorithms for Distorted Circular Contour Estimation", *IEEE trans. on IP*, vol 8, no 1, pp. 2369-2378, sept. 86.

[4] H. K. Aghajan and T. Kailath, "Sensor array processing techniques for super resolution multi-line-fitting and straight edge detection", *IEEE trans. on IP*, vol 2, no 4, pp. 454-465, Oct. 93.

[5] S. Bourennane and J. Marot, "Contour estimation by array processing methods", *Applied signal processing*, article ID 95634, 15 pages, 2006.

[6] J. Illingworth and J. Kittler, "A survey of the Hough transform", *Comput. Vis. Graph. IP*, no. 44, pp. 87-116, 88.